

Article

Quantitative Comparison of Infrared Thermography, Visual Inspection, and Electrical Analysis Techniques on Photovoltaic Modules: A Case Study

Leonardo Cardinale-Villalobos ^{1,*} , Carlos Meza ^{1,2} , Abel Méndez-Porras ³  and Luis D. Murillo-Soto ⁴ 

¹ Electronics Engineering School, Instituto Tecnológico de Costa Rica, Cartago 159-7050, Costa Rica; carlos.meza@hs-anhalt.de

² Department of Electrical, Mechanical and Industrial Engineering, Anhalt University of Applied Sciences, 06366 Köthen, Germany

³ Computer Engineering Department, Instituto Tecnológico de Costa Rica, Cartago 159-7050, Costa Rica; amendez@tec.ac.cr

⁴ Electromechanic Engineering School, Instituto Tecnológico de Costa Rica, Cartago 159-7050, Costa Rica; lmurillo@tec.ac.cr

* Correspondence: lcardinale@tec.ac.cr; Tel.: +506-2401-3221

Abstract: This paper compares multiple techniques to detect suboptimal conditions in the PV system. Detection of suboptimal conditions in the PV system is required to achieve optimal photovoltaic (PV) systems. Therefore, maintenance managers need to choose the most suitable techniques objectively. However, there is a lack of objective information comparing the effectiveness of the methods. This article calculates and compares the effectiveness of Infrared thermography (IRT), visual inspection (VI), and electrical analysis (EA) in detecting soiling, partial shadows, and electrical faults experimentally. The results showed that the VI was the best at detecting soiling and partial shading with 100% of effectiveness. IRT and EA had an effectiveness of 78% and 73%, respectively, detecting the three types of conditions under study. It was not possible to achieve maximum detection using only one of the techniques, but that VI must be combined with IR or EA. This research represents a significant contribution by achieving an objective comparison between techniques for detecting suboptimal conditions, being very useful to guide PV system maintainers and designers of fault detection techniques.

Keywords: solar PV system; fault detection performance; partial shading; soiling; electrical faults; thermography; electrical analysis



Citation: Cardinale-Villalobos, L.; Meza, C.; Méndez-Porras, A.; Murillo-Soto, L.D. Quantitative Comparison of Infrared Thermography, Visual Inspection, and Electrical Analysis Techniques on Photovoltaic Modules: A Case Study. *Energies* **2022**, *15*, 1841. <https://doi.org/10.3390/en15051841>

Academic Editor: Mohammadreza Aghaei

Received: 1 February 2022

Accepted: 24 February 2022

Published: 2 March 2022

Publisher's Note: MDPI stays neutral with regard to jurisdictional claims in published maps and institutional affiliations.



Copyright: © 2022 by the authors. Licensee MDPI, Basel, Switzerland. This article is an open access article distributed under the terms and conditions of the Creative Commons Attribution (CC BY) license (<https://creativecommons.org/licenses/by/4.0/>).

1. Introduction

In the area of PV systems engineering, an important topic is the operation, performance, and maintenance of PV Systems, that is, all the activities related to the monitoring, predictive and corrective maintenance, system failure analysis, system reliability, and operational safety.

PV Systems' benefits depend on their performance over their lifetime. Suboptimal conditions and faults such as electrical failures, partial shading, and soiling make the power delivered by solar modules decrease and may even generate irreversible damage [1]. There are design assumptions to avoid future suboptimal conditions such as partial shadows [2]; however, they can still occur in the future due to changes in surrounding installation factors. Therefore, it is critical to be able to detect these conditions effectively.

Using fault detection techniques it is possible to detect suboptimal conditions to act promptly before there is a significant impact on delivered power or a fire [3]. Research into fault detection techniques has led to their implementation in inverters [1], however there are still many limitations. In [4] a summary of the types of faults and available

techniques is made, among which, we can find visual inspection, the use of drones for infrared thermography [5] and the analysis of electrical variables such as power [6].

Efforts to make photovoltaic (PV) system maintenance more effective and efficient have led to the development of continuous monitoring systems and extensive research into fault detection techniques (e.g., [2,7]). However, a lack of quantitative information to assess its effectiveness has been identified as it is mentioned in [8]. In [9] an initial contribution to this situation was presented. In this case, a methodology was proposed to compare the effectiveness of failure detection of infrared thermography (IRT) and visual inspection (VI), however the electrical analysis (EA) technique was not considered.

This paper presents an extension of the work mentioned above. Besides IRT and VI, a third fault detection technique has been included, namely, EA, which detects faults by analyzing the estimated and actual electrical power. More specifically, the work assesses the effectiveness of IRT, VI, and EA to detect failures by partial shading (PS), soiling (S), and electrical faults (E). The previously mentioned faults are detailed in the next subsection. This research contributes to:

- the generation of quantitative indicators of effectiveness for failure identification methods, which are very limited or do not exist at the experimental level,
- a more detailed experimental characterization of each method, identifying strengths and limitations under different types of conditions,
- a more objective selection of the method(s) to be used at a PV installation for a more efficient operation and maintenance of the plant.

The rest of the paper is structured as follows: the following subsection presents the sub-optimal conditions considered. Section 2 describes the material and methods used. Section 3 presents the main results and discussion, and Section 4 describes the main conclusions. The list of nomenclatures and abbreviates are listed at the end of this document.

1.1. Related Work and Research Gap

Other works have characterized and compared fault detection techniques in order to understand the limitations and possibilities of each technique (see Table 1). Table 1 shows that the research developed so far for the comparison of techniques for the detection of suboptimal conditions has been based on literature reviews, without experimental evaluation. Experimental investigation has been done mainly on each particular method and under specific suboptimal conditions, which does not allow a direct comparison between the different techniques.

Table 1. Some relevant research related to the characterization or comparison of failure detection techniques.

Author	Research Description	Literature Review	Experimental Tests
[10]	Identifies the main faults in PV arrays and identifies detection techniques that can detect them	X	
[8]	Establishes a metric to compare fault detection techniques according to their capabilities for: (1) detection and classification, (2) real-time detection, (3) localization, (4) fault isolation.	X	
[3]	Compares fault detection techniques considering aspects such as: faults detected, level of diagnosis provided by the technique, on-line or off-line use, integration complexity and cost.	X	

Table 1. Cont.

Author	Research Description	Literature Review	Experimental Tests
[5]	Evaluates the possibilities of detecting failures by IRT and VI		X
[4]	Compares fault detection techniques considering, for example: required measurements, DC or AC type fault detection, type of technique and whether it was validated by simulation or experimentally.	X	
[11]	Determination of the effectiveness of a fault detection algorithm by means of an experiment inducing electrical faults.		X

Although there is previous research that characterizes or compares failure detection techniques, there is a lack of quantitative indicators that would allow a comparison to guide maintenance managers in choosing the most effective method. It was recently reviewed 40 failure detection techniques and found that quantitative indicators such as accuracy were lacking in order to make a better comparison between them [8]. This research specifically addresses the comparison of techniques for the detection of suboptimal conditions, based on an experimental approach, generating quantitative effectiveness indicators.

1.2. Suboptimal Conditions Considered

A suboptimal condition is a situation, event, or disturbance that causes a PV system to produce less than it could if that condition did not exist. In this paper, only the most common suboptimal conditions are considered, namely,

- **Partial shadowing:** A partial shadow on a PV array creates a specific region in which the irradiance is lower, resulting in a decrease in the power of the entire array [3]. Figure 1a shows a PV array with a shaded region due to a tree on the left, and Figure 1b shows a PV array with dirt on the PV module. Both cases cause a decrease in power, which will depend on the size and degree of shading [12,13].
- **Soiling:** The presence of dust, leaves, dirt, and generally any dirt will cause a decrease in the power generated by a solar array, which will be more significant as the amount of dirt increases [13]. Uniform dirt (evenly distributed dust) and non-uniform dirt (patches of dirt or bird drops) will have an affection on the power; the latter can also be classified as shading since it creates a decrease in the irradiance that affects the PV module, equivalent to a partial shade [14]. The effect on the power due to non-uniform dirt causes a hot spot to be formed [13]. Figure 2 shows a PV array with natural dirt, in which non-uniform dirt can be observed.
- **Electrical Faults:** From the electrical point of view, and according to [1], failures can be classified as (1) Ground faults, (2) Interline faults, (3) Open circuit faults, (4) others. It has been reported that faults cause a decrease in the power delivered and an increase in the temperature that varies according to the type of fault [8,15–17]. The following faults were applied in this investigation: short circuit in a PV module, ground fault, and open circuit. These are represented in Figure 3 with red lines.



Figure 1. (a) PV-chain with partial shade due to a tree, (b) PV-chain with dirt due to a bird drop.



Figure 2. Monocrystalline PV module analyzed with the presence of natural non-uniform dirt.

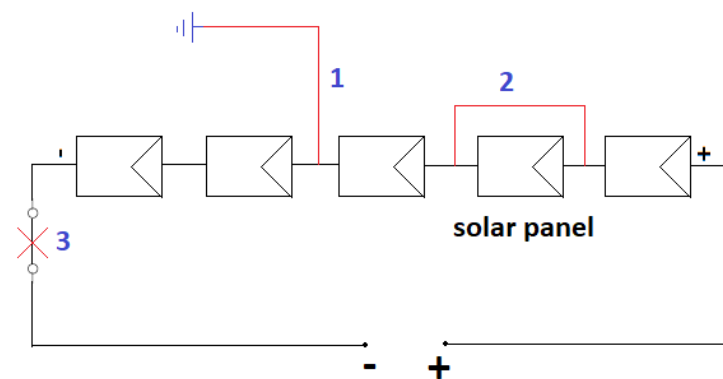


Figure 3. Types of electrical failures analyzed in this research. (1) Short circuit to ground, (2) Short circuit in PV module and (3) Open circuit.

2. Materials and Methods

This section details the installation, protocols, measuring instruments and the main methodological aspects used for the experimental tests.

2.1. The PV Installation Analyzed

The photovoltaic installation used is located in the northern part of Costa Rica, $10^{\circ}32'$ latitude and $-84^{\circ}31'$ longitude. According to the Köppen-Geiger system, the climate in this location is classified as tropical rainforest climate (Af). The PV plant it is located at the San Carlos Local Technological Campus in Santa Clara, Costa Rica. It is made up of six PV arrays, of which, three of monocrystalline technology were used for the development of the

experiment because the EA method is designed for monocrystalline modules. The details of the PV arrays used are shown in the Table 2.

Table 2. Information about the PV arrays under study.

Parameter	Value
Longitude	−84.51
Latitude	10.36
Azimuth angle	0° with respect to the South
Inclination angle	15°
Peak DC power (kW)	3.36
Number of PV modules	12
PV module models	Canadian Solar CS6k-280M
Total surface (m ²)	19.6
Date of commissioning	31 May 2017

The installation used in the research consists of 6 PV arrays of 12 monocrystalline and polycrystalline modules in series, each connected to a Sunny Boy 3000TL-US SMA inverter. The monocrystalline PV arrays selected for the experiment in this research are identified by the numbers 2, 4, and 6 in Figure 4.

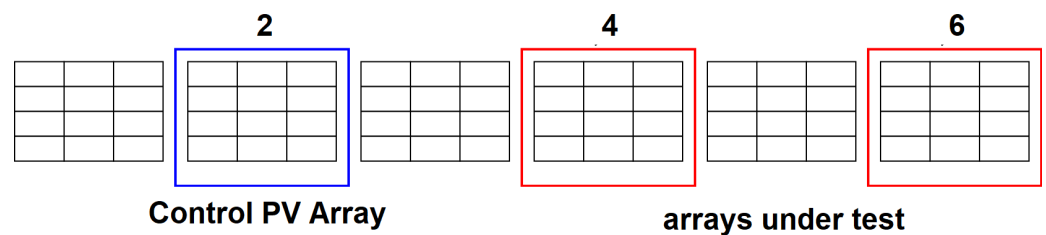


Figure 4. Diagram of the analyzed PV installation. The monocrystalline PV arrays 2, 4 and 6 were used in this research.

2.2. Protocol for the IRT and VI Missions

The procedure used was based on the one used by [9]. In this research, for each suboptimal condition, a flight was made with the UAV capturing RGB and infrared images of the PV chains. The flight height was set at 25 m, considering that this allows detecting possible failures with a resolution of the photovoltaic cell [9]. The irradiance was always higher than 700 W/m² with an angle around 20° from the PV module's perpendicular, the sky was clear and there were no wind currents. Emissivity was 0.85 for IRT. Consecutive images were taken every 1 s for the IRT and 2 s for the VI. The thermal images were configured to contain the radiometric information in RJPEG format.

For each test, the irradiance, ambient temperature and relative humidity were recorded. Each suboptimal condition was applied 15 min before the measurement was taken to ensure that thermal equilibrium existed [18].

2.3. Description for Electrical Measurements

This method was based on comparing the real generated power and the estimated theoretical power. The model used to estimate the generated power is the one proposed by [19]; the model starts from estimating the efficiency with Equation (1).

$$\eta_T(T, G) = -765.231 \times 10^{-6} \cdot T + 7.484 \times 10^{-6} \cdot G + 182.712 \times 10^{-3} \quad (1)$$

For greater accuracy in the model, wiring and aging losses were included as shown below:

$$\eta_l(T, G) = \eta_T(T, G)(1 - l_w)(1 - l_y) \quad (2)$$

where, $l_w = 0.01$ and represents the electrical wiring losses and $l_y = 0.03625$ represents the aging losses according to the manufacturer's information. Then, in order to calculate the power and compare it with the power measured in the inverters, Equation (4) was used.

$$P(T, G) = 12 \cdot A_p \cdot G \cdot \eta_l(T, G) \quad (3)$$

Finally, the system was tested under normal conditions to be empirically calibrated using the control PV array (string 2), so a correction factor k was applied, and a constant a was added to obtain the equation used by the EA method:

$$P_E(T, G) = 1.0111 \cdot P(T, G) - 35.734 \quad (4)$$

When applying each suboptimal condition, it was waited at least 5 min to take the measurements of the required physical variables, ensuring that the measurement corresponds to the steady-state of the failure. In order to establish this parameter, it was considered that in case of a variation in the PV array conditions (e.g., a failure), the inverter takes time to reach the stability of the new operation point [20], although this time can be less than 1 s, it was decided to leave a longer time.

Each measurement was obtained from the average of 1 min to have a measurement that was not affected by external fluctuations, namely: (a) sudden changes in weather conditions and (b) difference between the sampling times of the real power and the variables to estimate the theoretical power.

2.4. Fault Detection Criteria

The criteria used for the detection of suboptimal conditions were established from the review of scientific literature with experimental information. Taking [21,22] as a reference, the suboptimal conditions for infrared thermography considered were: (1) hot spot with a temperature differential of 10 °C or more, (2) PV string with a differential of 3.5 °C or more. For VI, the detection of shadows or dirt was established as a criterion [23]. For the electrical analysis, a power drop of 4% or more was considered as a suboptimal condition [24].

Table 3 details the suboptimal detection criteria used in the experiment.

Table 3. Criteria used for each technique evaluated to detect the failures induced from each suboptimal condition.

Technique	Criteria for Fault Detection
IRT	Hot spot with a delta ≥ 10 °C
	PV-chain with a temperature delta 3.5 °C in relation to a neighboring chain
VI	Presence of radiation attenuation on the PV module due to shade
	Appearance of light or heavy soiling
EA	Reduction of 4% or more compared to the theoretical power

2.5. Instrumentation

Figure 5 shows a diagram of the instruments used for the experiment. Below the many characteristics of the instruments and equipment used:

- Drone Phantom 4 Pro with a FLIR VUE PRO R 336 thermal camera (see Figure 6).
- The RGB camera used for the VI has the following features: 1" CMOS sensor, lens with an 84° FOV of 8.8 mm/24 mm, 4096 × 2160 resolution, JPEG format images, image size of 3:2; 4:3; 16:9 and an ISO range of 100–3200 (auto).
- The thermal camera has an uncooled microbolometer sensor, specifications are in [25,26], which are: HFOV × VFOV of 25° × 19°, 5.764 mm × 4.351 mm sensor, 13.00 mm focal

length, 336×256 resolution, 9 Hz frequency, accuracy of $\pm 5^\circ\text{C}$ or 5% from reading and thermal sensitivity of 40 mK.

- Vantage Pro2 Weather Station with temperature sensor to measure the ambient temperature required for thermogram analysis. The accuracy of the temperature sensor is $\pm 0.3^\circ\text{C}$.
- Spektron 210 pyranometer to verify that minimum irradiance conditions are met and to apply the EA method. The accuracy is $\pm 5\%$ of the annual measurement of the annual mean.
- Invert for the measurement of real power required by the EA. Accuracy is class 0.5 in accordance with ANSI C12.20.
- Digital contact temperature sensor model DS18B20 to apply the EA. Accuracy is $\pm 0.5^\circ\text{C}$.

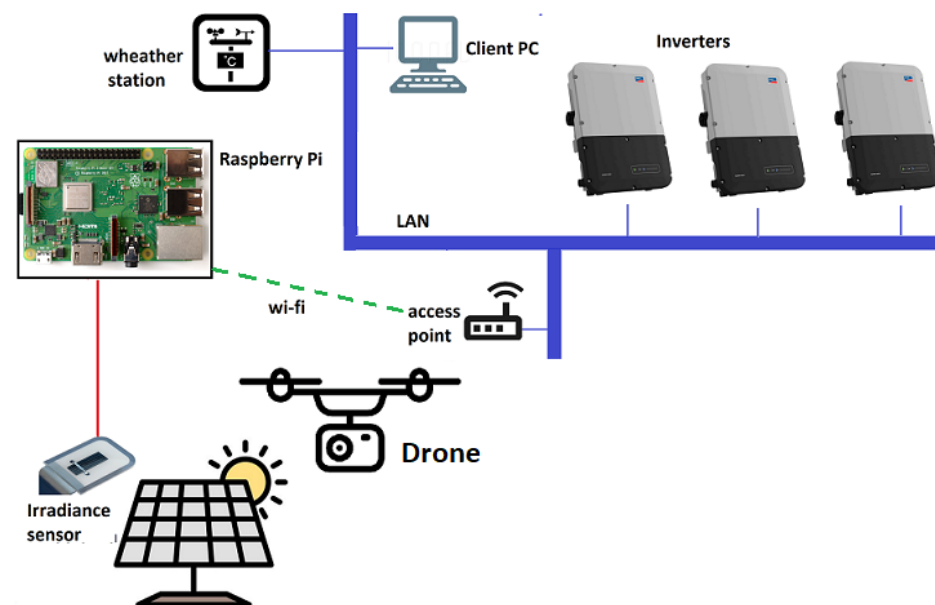


Figure 5. Schematic diagram of the instrumentation and communication links used to access the information sources of the experiment.



Figure 6. Side (left) and front (right) view of the UAV with infrared and RGB cameras used in the investigation.

2.6. Experiments

An experiment was developed by inducing the suboptimal conditions of interest and the three fault detection techniques were applied to each one.

The experiment used a repeated measurement design because multiple suboptimal conditions had to be applied to the same PV array [27]. A total of 28 cases were analyzed from the 11 suboptimal conditions applied to the two PV arrays. (Strings 4 and 6). String 2

was used as a control subject to establish a reference condition in each case for the normal operation of the PV strings, i.e., without applying failures. The factors and levels evaluated are shown in Table 4.

Table 4. Factors (types of failures) and levels used to generate the diverse suboptimal conditions to be evaluated in the experiment.

Suboptimal Condition	Factor	Level
S1	Soiling	10 months of natural soil
S2		30 months of natural soil
S3		12 cells with white spots
S4		12 cells with dry leaves from the site
S5		21 cells with white spots
S6		21 cells with dry leaves from the site
PS1	Partial shading	Shading of approximately 70% of a module's area
PS2		2 shadows, each approximately 30% of the area of a module
E1	Electrical fault	Short circuit in module
E2		Ground fault in second module
E3		Open circuit in the array

The suboptimal conditions were applied to the PV arrays without interaction between the type of suboptimal conditions analyzed. Each level was applied in both PV arrays making two repetitions (Except S1 and S2, which were each applied to a single PV array because it was natural soiling). The selection of the modules of each string to which the failure was applied was chosen at random. It was assumed that there is an independent relationship between the suboptimal conditions because they were randomized and did not generate a residual effect in the PV array [28], i.e., the PV string returned to their normal state once the suboptimal condition is removed. Each of the suboptimal conditions are described in the following section.

2.7. Description of Each Factor and the Levels of the Experiment

To continue the work started by [29], the same suboptimal conditions of soiling and partial shading were used, and the suboptimal conditions corresponding to electrical failures were included. Each is described in this section.

- A. Soiling

Six soiling conditions were used; these are identified as S1-S6 in Table 4. The suboptimal conditions S3 and S5 were prepared by applying white paint to the glass. Suboptimal conditions S4 and S6 used leaves and seeds found on-site around the solar PV modules. These suboptimal conditions are described as strong shading [13]. The glasses used to emulate the soiling condition are described in detail in [29].

- B. Partial shading

The PS1 and PS2 suboptimal conditions generated a natural shade allowing the incidence of diffuse radiation [30]. For this, an object was placed next to the PV array (see Figure 7) at 9:30 a.m. for PS1 and at 10:30 a.m. for PS2.



Figure 7. Object used to generate partial shade conditions. The shadow generated corresponds to the PS1 suboptimal condition.

- C. Electrical faults

In previous research work, electrical failures were evaluated at the experimental level by modifying the electrical connections of the PV system, e.g., open circuits and short circuits. Using [31] as a reference, switches were installed in the study PV arrays to emulate that effect; an electrical diagram of how this was implemented is shown in Figure 8. The E1 suboptimal conditions was randomly located in each of the evaluated cases. E2 was applied, maintaining the fixed position to generate a short circuit at a low voltage and not to expose the circuit to electric arcs. The E3 suboptimal conditions has the same effect in any location due to all the modules' series circuit configuration. Therefore, the location of the switch was not changed.

2.8. Date and Conditions of the Experiment

The IRT and VI measurements were made between 18 August and 2 September 2020. EA measurements were made between 17 September and 30 October. The average ambient temperature was 30 °C, the relative humidity 60%, and the reflected temperature 22 °C.

2.9. Power Normalizing

A comparison was made of the average power generated between the study PV arrays (strings 4 and 6) and the control PV array (string 2). The measurement was made during two hours with an irradiance greater than 700 W/m². A difference of 0.67% and −0.59% was obtained for strings 4 and 6, respectively. These results allowed us to consider that the strings are equivalent.

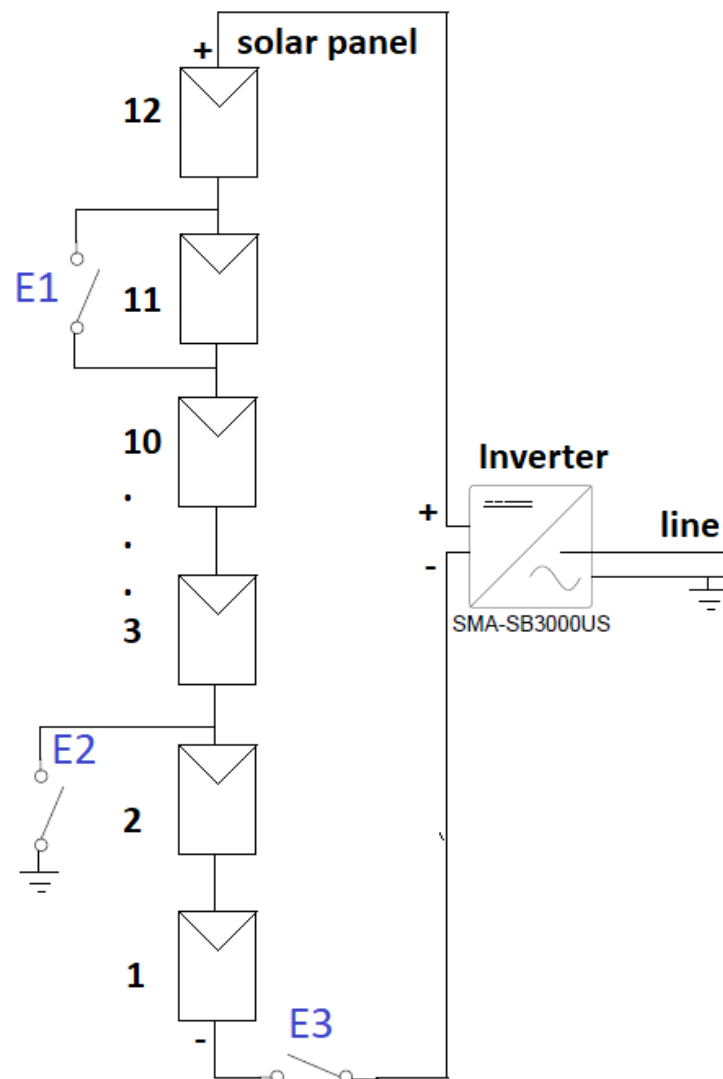


Figure 8. Diagram of the location of the switches used to generate the electrical suboptimal conditions evaluated in the experiment.

3. Results and Discussion

3.1. Power Affect for Each Case Evaluated in the Experiment

Each suboptimal condition was applied to the study PV arrays (strings 4 and 6) and was compared with the control PV array (string 2); with this, it was verified that all the cases had an affectation of at least 4%, i.e., that it met the criteria of failure. The results are shown in Table 5; these considered the normalization of the power measurements with respect to the reference array [29].

3.2. Results of the Experiment

For each case evaluated, a discrete output variable was generated to indicate whether or not the technique detected failure; the results are shown in Table 6. This table incorporates the VI and IRT measurements that had been reported by [29] for consideration in this new analysis.

Table 5. Validation of the effect on power of each of the suboptimal conditions evaluated in the experiment.

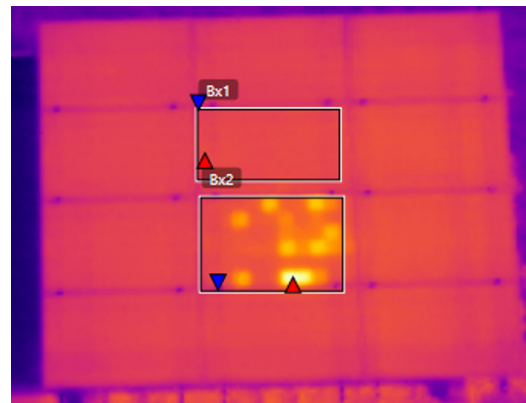
Case Evaluated	Irradiance W/m ²	Reference Array Power (W)	Tested Array Power (W)	Power Reduction	Fault (Yes/No)
1	783	2148	1885	12%	Yes
2	783	2148	1472	31%	Yes
3	724	2126	1872	12%	Yes
4	724	2126	1449	32%	Yes
5	775	2528	1876	26%	Yes
6	887	2883	1915	34%	Yes
7	836	2671	2150	20%	Yes
8	1040	3421	2541	26%	Yes
9	984	3086	2593	16%	Yes
10	943	3077	2066	33%	Yes
11	1059	3285	2884	12%	Yes
12	956	3201	2141	33%	Yes
13	971	3197	2611	18%	Yes
14	866	2911	2215	24%	Yes
15	873	2897	2399	17%	Yes
16	944	3077	2288	26%	Yes
17	890	2839	2366	17%	Yes
18	868	2841	2370	17%	Yes
19	1041	3416	2892	15%	Yes
20	793	2533	2091	17%	Yes
21	782	2589	2148	61%	Yes
22	958	2662	1889	34%	Yes
23	887	2582	2146	61%	Yes
24	1035	3045	2586	26%	Yes
25	782	2601	246	18%	Yes
26	892	2870	721	75%	Yes
27	887	2582	2127	18%	Yes
28	1079	2890	2207	24%	Yes
29	1030	2904	0	100%	Yes
30	1238	3226	0	100%	Yes
31	1030	2904	0	100%	Yes
32	1033	2814	0	100%	Yes
33	907	2637	2435	7%	Yes
34	949	2662	2458	8%	Yes
35	1053	2832	0	100%	Yes
36	996	2622	0	100%	Yes
37	906	2637	2348	8%	Yes
38	949	2662	2446	11%	Yes
39	1027	2743	0	100%	Yes
40	998	2637	0	100%	Yes

Table 6. Summary of the results of the experiment. D = Detected, ND = Not detected, NA = Not apply, S = soiling, PS = partial shading and E = electrical fault.

Case	Factor	Suboptimal Condition	IRT Result	VI Result	EA Result
1	S	S1	D	D	D
2	S	S2	ND	D	D
3	S	S1	D	D	D
4	S	S2	ND	D	D
5	S	S4	ND	D	D
6	S	S6	D	D	D
7	S	S4	D	D	ND
8	S	S6	D	D	D
9	S	S4	D	D	ND
10	S	S6	ND	D	D
11	S	S4	D	D	ND
12	S	S6	D	D	D
13	S	S5	ND	D	D
14	S	S3	ND	D	D
15	S	S5	ND	D	ND
16	S	S3	D	D	D
17	S	S5	D	D	ND
18	S	S3	D	D	ND
19	S	S5	ND	D	ND
20	S	S3	ND	D	ND
21	PS	PS1	D	D	ND
22	PS	PS2	D	D	D
23	PS	PS1	D	D	D
24	PS	PS2	D	D	D
25	PS	PS1	D	D	D
26	PS	PS2	D	D	D
27	PS	PS1	D	D	D
28	PS	PS2	D	D	D
29	E	E2	D	NA	D
30	E	E2	D	NA	D
31	E	E2	D	NA	D
32	E	E2	D	NA	D
33	E	E1	D	NA	ND
34	E	E1	D	NA	D
35	E	E3	D	NA	D
36	E	E3	D	NA	D
37	E	E1	D	NA	ND
38	E	E1	D	NA	D
39	E	E3	D	NA	D
40	E	E3	D	NA	D

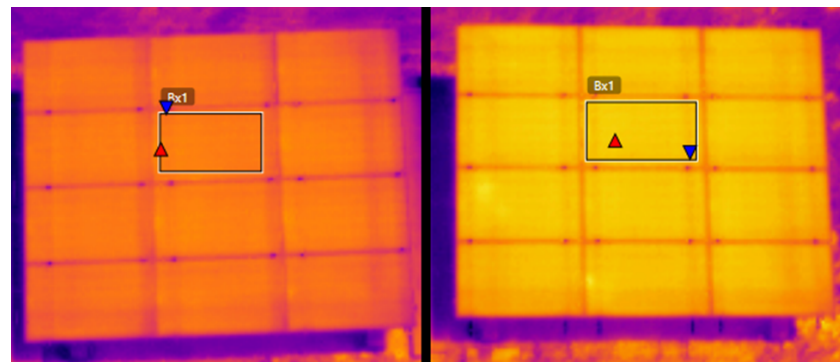
3.3. Image Analysis

Each case evaluated was analyzed manually for IRT and VI. The thermographs were processed with Flir Tools 5.13, and the RGB images were analyzed with traditional photo viewing software. Figures 9–11 show some electrical failures analyzed with IRT. Employing the VI, it was not possible to detect electrical failures.



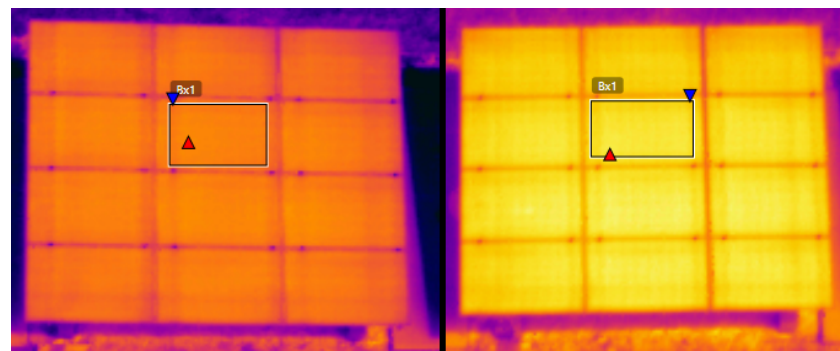
Temperature delta > 10 °C

Figure 9. IR image analyzed for case 37. In this one, the heating generated in a solar PV module due to the presence of a short circuit is observed.



Temperature difference between strings $\geq 3.5^{\circ}\text{C}$

Figure 10. IR images analyzed for case 39. String 2 (left) and string 6 (right). In this one, it can be seen that string 6 had a higher temperature than the control PV array (string 2) due to the open circuit.



Temperature difference between strings $\geq 3.5^{\circ}\text{C}$

Figure 11. IR images analyzed for case 30. String 2 (left) and string 4 (right). In this case, the short circuit to earth caused the inverter to open the circuit (electrical protection), causing an increase in the temperature of the entire string.

3.4. EA Analysis

Table 7 shows the detail of the measurements with the EA. It is observed that for all types of failures, in some cases, the failure was not detected; this is due to the fact that the estimated power was less than it should be under conditions without failure (cases 18, 21, and 33). Also, cases were found in which the estimated power affect deviated by less than 1% from the criteria for detecting failure (cases 13, 19, 20, and 34); which shows that accuracy errors of less than 1% will affect the effectiveness of the technique. This requires high precision in the instrumentation, in the parameters of the mathematical model, and in the processing of the information, with their respective experimental validation.

Table 7. Electrical measurements for the evaluation of each suboptimal condition with the EA technique. The last column on the right indicates the output variable of this method.

Case	Irradiance (W/m ²)	Tested Array Avg Temp. (°C)	Tested Array Power (W)	Estimate Power (W)	Power Reduction	Fault (Yes/No)
1	783	50.4	1885	2191	14.0%	Yes
2	783	52.5	1472	2167	32.1%	Yes
3	724	50.5	1872	2015	7.1%	Yes
4	724	52.3	1449	1996	27.4%	Yes
5	775	56.9	1876	2092	10.3%	Yes
6	887	57.5	1915	2407	20.5%	Yes
7	836	57.8	2236	2258	1.0%	No
8	1040	53.6	2541	2910	12.7%	Yes
9	984	59.0	2593	2668	2.8%	No
10	943	49.0	2066	2686	23.1%	Yes
11	1059	57.1	2884	2914	1.0%	No
12	956	51.0	2141	2697	20.6%	Yes
13	971	52.0	2611	2728	4.3%	Yes
14	866	49.1	2215	2454	9.7%	Yes
15	873	53.0	2399	2424	1.0%	No
16	944	48.9	2288	2688	14.9%	Yes
17	890	57.0	2366	2423	2.3%	No
18	868	58.5	2370	2339	-1.3%	No
19	1041	48.9	2892	2985	3.1%	No
20	793	55.5	2091	2163	3.3%	No
21	782	56.5	2148	2118	-1.4%	No
22	958	60.3	1889	2574	26.6%	Yes
23	887	55.1	2146	2437	12.0%	Yes
24	1035	59.4	2664	2808	5.1%	Yes
25	782	57.8	246	2102	88.3%	Yes
26	892	54.0	721	2468	70.8%	Yes
27	887	54.2	2127	2449	13.2%	Yes
28	1079	56.6	2207	2980	26.0%	Yes
29	1030	55.0	0	2858	100.0%	Yes
30	1238	59.0	0	3408	100.0%	Yes
31	1030	57.0	0	2828	100.0%	Yes
32	1033	58.0	0	2822	100.0%	Yes
33	907	62.8	2435	2396	-1.6%	No
34	949	58.2	2458	2578	4.7%	Yes
35	1053	56.0	0	2913	100.0%	Yes
36	996	57.0	0	2730	100.0%	Yes
37	906	63.2	2348	2388	1.7%	No
38	949	54.7	2446	2626	6.9%	Yes
39	1027	56.0	0	2837	100.0%	Yes
40	998	55.0	0	2765	100.0%	Yes

Cases that were at 1% or less of the limit defined as criteria for failure detection are identified in light blue. Cases that showed an increase in power in the presence of the fault were marked in green.

3.5. Comparison of the Three Techniques

Considering that visual inspection does not detect the electrical faults examined, we initially compared the effectiveness of the techniques for detecting soiling and partial shading; this is shown in Figure 12. It was found that IV achieved the maximum effectiveness (100%), outperforming the other two techniques (68% each). These results reinforce the findings found in [29] on the high effectiveness of VI in detecting this type of failure

concerning other techniques. Comparing the number of cases detected by IRT and EA shows that EA outperformed IRT in the soiling tests but had lower performance in the partial shadowing tests.

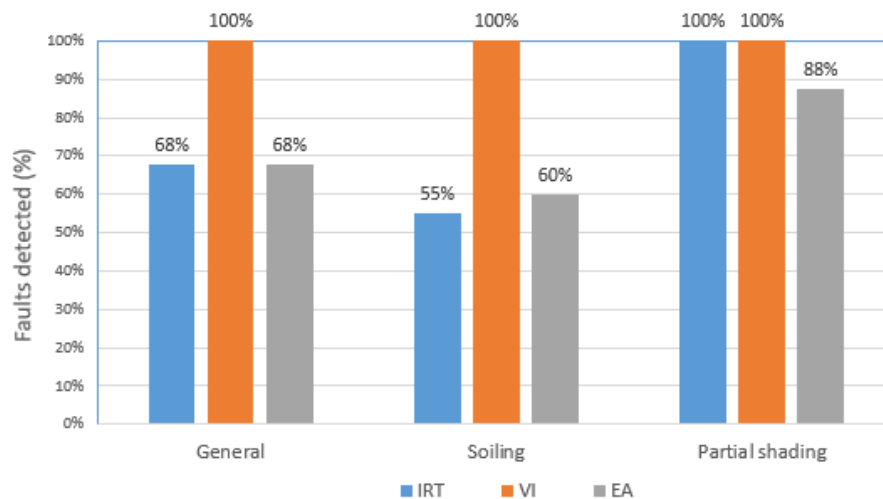


Figure 12. Percentage of failures detected by the techniques under study for soiling and partial shading conditions.

Figure 13 shows the number of failures detected for IRT and EA for the three types of failures studied in this research. It can be observed that, in general, the IRT detected more faults, being surpassed by EA only for soiling detection.

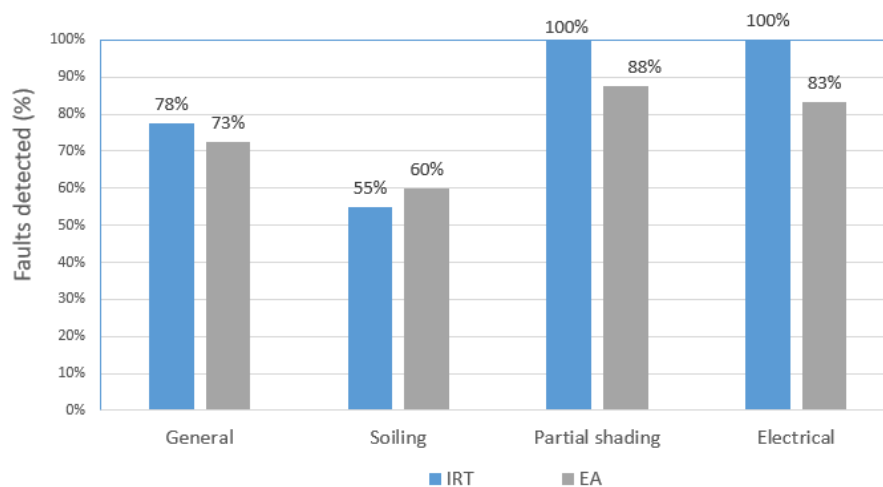


Figure 13. Percentage of failures detected by IRT and EA for the three types of failures analyzed in this research.

From Figures 12 and 13 it can be seen that in general, soiling is the type of condition that was least detected, while partial shading was the most detected. Electrical faults were also mainly detected; however, it should be considered that VI does not work for this type of fault.

Considering the output variable of continuous type (1 = detected and 0 = not detected), an analysis of the variance was made. The variances were 0.219, 0.0417, and 0.0797 for the soiling, partial shading, and electrical faults, respectively. This indicates that the detection of soiling faults had greater variability. The high variability detecting soiling indicates that more research should be done focused on improving the effectiveness of IRT and EA detecting soiling.

Figure 14 shows the results of soiling detection by EA, in which it can be seen that all types of soiling were detected at least in a low percentage of occasions. This indicates that the EA technique does detect the types of soiling evaluated but with less effectiveness. The reasons why, in some cases, this type of failure was detected and in others not, requires a more detailed study specifically on this subject. This compartment had also been identified for IRT detecting soiling [29].

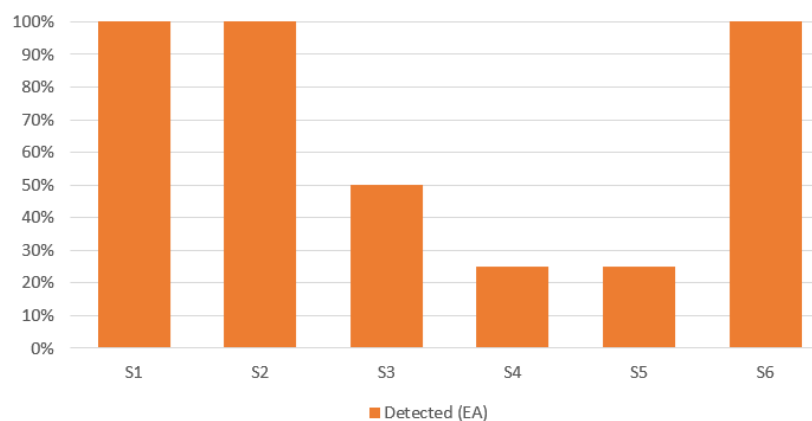


Figure 14. Percentage of soiling failures that were detected by the EA. S1 and S2 were applied twice, the other four times.

The only technique based on qualitative criteria for the detection of failures was the VI, which implies that its effectiveness could be affected due to the subjectivity that could exist before other types of failures. Therefore, the definition of quantitative criteria for the VI is an area that could vary the technique's performance for certain types of failures.

From Table 6 it can be seen that each of the suboptimal conditions that were evaluated were detected by at least one of the failure detection techniques. Therefore, for the suboptimal conditions evaluated and the techniques used, combining them is the way to achieve maximum detection.

3.6. Statistical Hypothesis Testing

Using contingency tables and Fisher's exact test, the effectiveness of the techniques can be evaluated by comparing them in pairs [32,33]. To determine if there is a significant difference between the total number of failures detected by each technique, the following hypothesis tests were defined: as follows:

$$H_{0,1} : N_i = N_j$$

$$H_{a,1} : N_i \neq N_j$$

$$H_{0,2} : N_i = N_k$$

$$H_{a,2} : N_i \neq N_k$$

$$H_{0,3} : N_j = N_k$$

$$H_{a,3} : N_j \neq N_k$$

$$\forall i \neq j \neq k$$

where N is the number of identified failures, i , j , and k are IRT, VI, and EA techniques, respectively. Table 8 shows the p -values obtained for each hypothesis test.

Table 8. p -value obtained for each of the hypotheses evaluated.

Hypothesis	p -Value
$H_{0,1}$	0.001
$H_{0,2}$	0.797
$H_{0,3}$	0.002

Considering a significance level $\alpha = 0.05$ because no major requirement has been identified [34], the hypotheses $H_{0,1}$ and $H_{0,3}$ are rejected; that is, significant differences were found between the number of faults detected. Each of the techniques was also compared for the different types of failure applied, for which p -value $< \alpha$ and odd ratio (OR) was obtained for the cases shown in Table 9.

Table 9. p -value less than α and OR obtained by analyzing significant differences for each type of failure.

Technique 1–Technique 2	Type of Fault	p -Value	OR
EA-VI	S	0.003	27.88
IRT-VI	S	0.001	33.9 *

* The order of the column in the contingency table was changed to achieve OR > 1 .

From the analysis of Tables 8 and 9, it was interpreted which method was better than another for each type of failure; this is summarized in Table 10. The OR coefficients shown indicate that, in addition to accepting the alternative hypotheses for these types of failure, there is a high probability that the technique will succeed in detecting a failure of this type compared to the other technique [35].

Table 10. Significant differences in the detection of each type of failure between the methods studied. Note: The types of failures not indicated had no significant differences.

Techniques	Result
EA-VI	VI detects soiling better
IRT-VI	VI detects soiling better
IRT-EA	No significant differences were found

4. Conclusions

The effectiveness of IRT and EA detecting soiling, partial shading and electrical faults was 78% and 73% respectively. Comparing the three techniques, it was determined that to detect soiling and partial shadows, VI is the most effective technique; reaching 100% effectiveness for the suboptimal conditions under study. However, we cannot say that this technique in general terms is better than the other two, as VI could not be used to detect electrical faults. It should also be considered that there are multiple techniques for fault detection by means of electrical analysis, one of them was used in this study. The effectiveness of other techniques by electrical analysis remains to be studied.

Analyzing each type of failure, significant differences were found for the VI. This was the best technique detecting soiling (100%) in comparison to IRT (55%) and EA (60%). In addition, partial shadows were the type of fault that was mostly detected by all the techniques, finding that none of the techniques is more effective than the others for this failure.

When comparing these results with those found in [29], it is identified that the calculated effectiveness depends on the design of the experiment, therefore, the procedures of each technique, the criteria for detection of failures and the suboptimal conditions to be evaluated, must be carefully selected and documented in detail to support the results found.

The determination of the effectiveness of EA detecting soiling showed that the same suboptimal condition can be detected in some cases and not in others, therefore, this type

of failure can be analyzed in more detail using this methodology increasing the replication of the suboptimal conditions to increase the statistical power.

For maximum detection of suboptimal conditions such as those studied in this research, VI should be combined with IRT or EA, using only one of the techniques will leave failures undetected and it was not found necessary to combine EA with IRT, since both have equivalent effectiveness. It is still pending to make a comparison around other capabilities of the techniques, for example, the location and identification of faults.

The results obtained in this work allow a quantitative comparison of the effectiveness of IRT, EA, and VI techniques, which contributes to mitigating a knowledge gap detected in this area. Furthermore, it contributes to improving fault detection techniques since information regarding the strengths and limitations of each of them has been obtained experimentally. Moreover, future work that combines the methods mentioned above can improve existing fault detection techniques under challenging conditions, for instance, when a high level of diffuse irradiance is present.

Author Contributions: Conceptualization, C.M.; Investigation, L.C.-V.; Methodology, A.M.-P.; Supervision, L.D.M.-S. and C.M. All authors have read and agreed to the published version of the manuscript.

Funding: This research was funded by the Vice Rector's Office for Research and Extension of the Costa Rica Institute of Technology, grant number 5402-1360-4201.

Institutional Review Board Statement: Not applicable.

Informed Consent Statement: Not applicable.

Data Availability Statement: Not applicable.

Conflicts of Interest: The authors declare no conflict of interest.

Nomenclature and Abbreviates

Symbol	Quantity	Unit/Value
η_T	Electrical efficiency	%
η_l	Electrical efficiency with wiring and aging losses	%
P	Electrical efficiency with losses	W
P_E	Calibrated electrical efficiency of the array	W
T	Cell temperature	°C
G	Irradiance	W/m ²
A_p	Array area	m ²
k	Experimental efficiency correction factor	1.0111
a	Experimental efficiency correction constant	−35.73%
I_w	Wire losses	0.01
I_y	Aging losses	0.0365
HFOV	Horizontal Field of View	°
VFOV	Vertical Field of View	°
α	Significance level	0.05
Abbreviaton	Description	
PV	Photovoltaic	
IRT	Infrared thermography	
VI	Visual inspection	
EA	Electrical analysis	
PS	Partial shading	
S	Soiling	
E	Electrical Faults	
UAV	Unmanned Aerial Vehicle	
RGB	Red, green and blue	
S1	Soiling condition 1	

S2	Soiling condition 2
S3	Soiling condition 3
S4	Soiling condition 4
S5	Soiling condition 5
S6	Soiling condition 6
PS1	Partial shading condition 1
PS2	Partial shading condition 2

References

- Zhao, Y. *Fault Detection, Classification and Protection in Solar Photovoltaic Arrays*; Technical Report; Northeastern University: Boston, MA, USA, 2015.
- Zsiborács, H.; Zentkó, L.; Pintér, G.; Vincze, A.; Baranyai, N.H. Assessing shading losses of photovoltaic power plants based on string data. *Energy Rep.* **2021**, *7*, 3400–3409. [[CrossRef](#)]
- Mellit, A.; Tina, G.; Kalogirou, S. Fault detection and diagnosis methods for photovoltaic systems: A review. *Renew. Sustain. Energy Rev.* **2018**, *91*, 1–17. [[CrossRef](#)]
- Madeti, S.R.; Singh, S. A comprehensive study on different types of faults and detection techniques for solar photovoltaic system. *Sol. Energy* **2017**, *158*, 161–185. [[CrossRef](#)]
- Zefri, Y.; ElKettani, A.; Sebari, I.; Lamallam, S.A. Thermal Infrared and Visual Inspection of Photovoltaic Installations by UAV Photogrammetry—Application Case: Morocco. *Drones* **2018**, *2*, 41. [[CrossRef](#)]
- Murillo-Soto, L.D.; Meza, C. Diagnose Algorithm and Fault Characterization for Photovoltaic Arrays: A Simulation Study. In *Lecture Notes in Electrical Engineering*; Springer International Publishing: Base, Switzerland, 2020; pp. 567–582. [[CrossRef](#)]
- Corrales, D.; Cardinale-Villalobos, L.; Meza, C.; Murillo-Soto, L.D. Detection of Suboptimal Conditions in Photovoltaic Installations for Household-Prosumers; In Proceedings of the International Conference on Sustainable Smart Cities and Territories, Doha, Qatar, 27–29 April 2021; pp. 26–36. [[CrossRef](#)]
- Appiah, A.Y.; Zhang, X.; Ayawli, B.B.K.; Kyeremeh, F. Review and Performance Evaluation of Photovoltaic Array Fault Detection and Diagnosis Techniques. *Int. J. Photoenergy* **2019**, *2019*, 6953530. [[CrossRef](#)]
- Cardinale-Villalobos, L.; Rimolo-Donadio, R.; Meza, C. Solar Panel Failure Detection by Infrared UAS Digital Photogrammetry: A Case Study. *Int. J. Renew. Energy Res. (IJRER)* **2020**, *10*, 1154–1164.
- Alam, M.K.; Khan, F.; Johnson, J.; Flicker, J. A Comprehensive Review of Catastrophic Faults in PV Arrays: Types, Detection, and Mitigation Techniques. *IEEE J. Photovoltaics* **2015**, *5*, 982–997. [[CrossRef](#)]
- Zhao, Y.; Ball, R.; Mosesian, J.; de Palma, J.F.; Lehman, B. Graph-Based Semi-supervised Learning for Fault Detection and Classification in Solar Photovoltaic Arrays. *IEEE Trans. Power Electron.* **2015**, *30*, 2848–2858. [[CrossRef](#)]
- Mäki, A.; Valkealahti, S. Power Losses in Long String and Parallel-Connected Short Strings of Series-Connected Silicon-Based Photovoltaic Modules Due to Partial Shading Conditions. *IEEE Trans. Energy Convers.* **2012**, *27*, 173–183. [[CrossRef](#)]
- Maghami, M.R.; Hizam, H.; Gomes, C.; Radzi, M.A.; Rezadad, M.I.; Hajighorbani, S. Power loss due to soiling on solar panel: A review. *Renew. Sustain. Energy Rev.* **2016**, *59*, 1307–1316. [[CrossRef](#)]
- Javed, W.; Wubuliksimu, Y.; Figgis, B.; Guo, B. Characterization of dust accumulated on photovoltaic panels in Doha, Qatar. *Sol. Energy* **2017**, *142*, 123–135. [[CrossRef](#)]
- Chaudhary, A.S.; Chaturvedi, D. Analyzing Defects of Solar Panels under Natural Atmospheric Conditions with Thermal Image Processing. *Int. J. Image Graph. Signal Process.* **2018**, *10*, 10–21. [[CrossRef](#)]
- Tsanakas, J.A.; Ha, L.; Buerhop, C. Faults and infrared thermographic diagnosis in operating c-Si photovoltaic modules: A review of research and future challenges. *Renew. Sustain. Energy Rev.* **2016**, *62*, 695–709. [[CrossRef](#)]
- Wang, Y.; Itako, K.; Kudoh, T.; Koh, K.; Ge, Q. Voltage-Based Hot-Spot Detection Method for Defective Cell in Photovoltaic Module Using Projector. *J. Energy Power Eng.* **2016**, *10*, 489–496. [[CrossRef](#)]
- International Energy Agency. *Review on Infrared and Electroluminescence Imaging for PV Field Applications*; Technical Report; Photovoltaic Power Systems Programme; IEA: Paris, France, 2018.
- Murillo-Soto, L.; Meza, C. Fault detection in solar arrays based on an efficiency threshold. In Proceedings of the 2020 IEEE 11th Latin American Symposium on Circuits Systems (LASCAS), San Jose, CA, USA, 25–28 February 2020; pp. 1–4. [[CrossRef](#)]
- Pradhan, R.; Panda, A. Performance evaluation of a MPPT controller with model predictive control for a photovoltaic system. *Int. J. Electron.* **2020**, *107*, 1543–1558. [[CrossRef](#)]
- Moretón, R.; Lorenzo, E.; Narvarte, L. Experimental observations on hot-spots and derived acceptance/rejection criteria. *Sol. Energy* **2015**, *118*, 28–40. [[CrossRef](#)]
- International Energy Agency. *Review of Failures of Photovoltaic Modules*; Technical Report; Performance and Reliability of Photovoltaic Systems; IEA: Paris, France, 2014.
- National Renewable Energy Laboratory. *Development of a Visual Inspection Data Collection Tool for Evaluation of Fielded PV Module Condition*; NREL: Golden, CO, USA, 2012.
- Acciani, G.; Falcone, O.; Vergura, S. Typical defects of PV-cells. In Proceedings of the 2010 IEEE International Symposium on Industrial Electronics, Bari, Italy, 4–7 July 2010; pp. 2745–2749. [[CrossRef](#)]
- Flir.com. *Adjusting Sensitivity & Gain on the FLIR Vue Pro R*; FLIR: Boston, MA, USA, 2019.

26. Flir. *Flir Vue Pro and Flir Vue Pro R*; FLIR: Boston, MA, USA, 2019.
27. Tango, T. *Repeated Measures Design with Generalized Linear Mixed Models for Randomized Controlled Trials*; Taylor & Francis Group: Tokyo, Japan, 2017.
28. Gutiérrez-Pulido, H.; De la Vara-Salazar, R. *Análisis y Diseño de Experimentos*, 2nd ed.; McGraw-Hill Interamericana: Mexico City, Mexico, 2008.
29. Cardinale-Villalobos, L.; Meza, C.; Murillo-Soto, L.D. Experimental comparison of visual inspection and infrared thermography for the detection of soiling and partial shading in photovoltaic arrays. In Proceedings of the Third Ibero-American Congress, ICSC-Cities 2020, San José, Costa Rica, 9–11 November 2020. [[CrossRef](#)]
30. Mekki, H.; Mellit, A.; Salhi, H. Artificial neural network-based modelling and fault detection of partial shaded photovoltaic modules. *Simul. Model. Pract. Theory* **2016**, *67*, 1–13. [[CrossRef](#)]
31. Zhao, Y.; Lehman, B.; Ball, R.; Mosesian, J.; de Palma, J.F. Outlier detection rules for fault detection in solar photovoltaic arrays. In Proceedings of the 2013 Twenty-Eighth Annual {IEEE} Applied Power Electronics Conference and Exposition ({APEC}), Long Beach, CA, USA, 17–21 March 2013. [[CrossRef](#)]
32. Jones, J.B.; Schropp, M.A. Research fundamentals: Statistical considerations in research design: A simple person's approach. *Acad. Emerg. Med.* **2000**, *7*, 194–199. [[CrossRef](#)]
33. Bolboacă, S.D.; Jäntschi, L.; Sestraş, A.F.; Sestraş, R.E.; Pamfil, D.C. Pearson-Fisher Chi-Square Statistic Revisited. *Information* **2011**, *2*, 528–545. [[CrossRef](#)]
34. Ventura-León, J.L. El significado de la significancia estadística: Comentarios a Martínez-Ferrer y colaboradores. *Salud Pú. México* **2017**, *59*, 499. [[CrossRef](#)]
35. Mchugh, M.L. The odds ratio: Calculation, usage, and interpretation. *Biochem. Med.* **2009**, *19*, 120–126. [[CrossRef](#)]